

International Journal of Sustainable Energy Planning and Management

Methodology to design district heating systems with respect to local energy potentials, CO₂-emission restrictions, and federal subsidies using oemof

Mathias Kersten*, Max Bachmann, Tong Guo, Martin Kriegel

Hermann-Rietschel Institute, Chair of Building Energy Engineering, Technical University of Berlin, Marchstr. 4, 10587 Berlin, Germany

ABSTRACT

To combine a variety of different heat generating technologies, static design methods will not be sufficient to design future heat supply systems. New energy system design approaches are being developed with consideration of fluctuating renewable energy sources, different subsidy measures, as well as CO₂-emission reduction targets.

The motive of this study is to develop a new methodology to design and optimise an energy system considering these constraints. The methodology is developed based on the Open Energy Modelling Framework (oemof) and applied on a sub-urban region in northern Germany. Local specifics of energy source potentials are taken into account. It adapts the boundary conditions of a German federal funding program for innovative heat supply networks "Heating Network Systems 4.0." Federal funding restrictions of combined heat and power systems and self-consumption are also considered.

An economic optimisation was conducted considering a variety of energy sources. Cost optimal energy system design was computed regarding investments costs, energy prices and annual CO₂-emission restrictions. The integration of combined heat and power (CHP), photovoltaic (PV) and heat pump (HP) systems in combination with storage size optimisation can reduce CO₂-emission of heat production by approx. 69% compared to the current state of heat production.

Keywords

Sub-urban;
CO₂-emission reduction;
Design tool;
Economic optimisation;
Federal funding;

<http://doi.org/10.5278/ijsepm.6323>

1. Introduction

Simple static design approaches for heat supply systems cannot take fluctuating renewable energy sources, annual CO₂-emission restrictions, or complex federal funding mechanisms into account, in CHP electricity production or HP electricity supply for example. The optimal size of thermal energy storage (TES) or information about charging and discharging cycles cannot be determined either. TES can be beneficial for improved utilisation of least-cost technologies [1], thus the economic optimisation of an energy system is mainly dependent on these parameters and data.

The energy system is further affected by changing ambient temperature and grid supply temperatures. Both

significantly influence the efficiencies of heat producing units especially HP. A precise analysis of the electricity supply of HP systems could benefit these regarding lower CO₂-emission when compared with other systems [2]. The number of parameters cannot be considered using static design approaches to determine and design an optimal supply solution. To conduct an economic optimisation of the energy supply system a more detailed approach than the static design approach is necessary. There are a variety of tools for optimising energy systems, such as EnergyPlan [3] and several projects dealing with the investigation of heating and cooling distribution networks. An overview of 58 projects in the context of Horizon2020 is given by [4] which shows the

*Corresponding author - e-mail: mathias.kersten@tu-berlin.de

Abbreviations	
4GDH	4th-Generation District Heating
aux	auxiliary
BG	biogas
BM	biomass
BMWi	Federal Ministry for Economic Affairs and Energy (Bundesministerium für Wirtschaft und Energie)
cap	capacity
CHP	combined heat and power
cond	condensing
COP	coefficient of performance
ct	€cent
DHC	district heating and cooling
DHP	district heating plants
DHW	domestic hot water
EEG	Renewable Energy Sources Act (Erneuerbare-Energien-Gesetz)
FLH	full load hours
GT	geothermal
HP	heat pump
hr	high revenue
KWKG	Combined Heat and Power Law (Kraft-Wärme-Kopplungs-Gesetz)
LCOE	levelised costs of energy production
lr	low revenue
NG	natural gas
oemof	Open Energy Modelling Framework
P2H	power to heat (e.g. electrode boiler)
PV	photovoltaic
red	reduction
SPF	seasonal performance factor
TES	thermal energy storage
TRY	test reference year
WW	wastewater

importance of this topic on the path of lowering CO₂-emission in the district energy supply sector. As pointed out in [5] the future planning of energy systems will be deeply affected by the process of the transition to a decarbonised heat supply system. The work of [1] investigates four types of district heating plants (DHP) and the influences of taxation and subsidies of energy in Denmark, Norway, Sweden, and Finland. In [6] the investments and operation of an urban energy system considering the coupling of electricity, heating, and transport sectors is investigated, using the City of Gothenburg as an example. The work of [7] conducts a design study of a poligeneration system for an existing district heating and cooling (DHC) network, though without setting specific constraints for CHP funding mechanisms as requested for this investigation. The work of [8] is analysing options for 100% renewable urban districts with highest possible self-consume of

locally generated renewable energy, pointing out that the feasibility of developed concepts for a Dutch case study depend on possible subsidies.

The methodology in this study addresses the implementation of constraints in funding mechanisms for sector coupling technologies and 4th-Generation District Heating (4GDH) in Germany in particular, based on the idea of designing a smart energy system [9]. The main goal of this study is to develop a methodology to design an economically optimal producer park for a district heating supply network considering local specifics of the model area as well as requirements regarding the CO₂-emission reduction of heat production. This methodology considers local energy potentials and a variety of heat producing units, as well as time dependencies of renewable energy sources and unit efficiencies. A specific case study using the methodology is developed around a model region in northern Germany, close to the city of Bremen.

The methodology is based on oemof.solph which is part of oemof [10] an organisational framework for scientists in the field of energy system modelling addressing the new challenges of energy system modelling [11]. Furthermore, it was “... *hypothesized as a progressive tool to design a sector-coupled and renewable-based energy system ...*” [12] and contains various packages and functionalities to model and optimise complex energy systems. Among other things, the framework has been used to investigate the optimal storage capacity for a northern German region [13] as well as to investigate compressed air storage potentials in the German energy system [14].

To define and calculate an energy system the model generator oemof.solph [15] is applied. The energy system model is based on the graph theory [16] and each part of the energy system is represented by a node. oemof.solph distinguishes between two kinds of nodes, buses and components.

The energy system is represented by a linear equation system considering these nodes. A more detailed view on the equations of this system and its components is given in section 2.1. Further information of the mathematical background can be found in [15].

A load profile was created via a thermal building simulation framework developed at the TU Berlin which had been adapted to a model region (see section 2.2). To design an optimal producer park to supply the model area economical parameters and the potentials of renewable energy sources within the model area are needed.

As necessary input data, the potentials of renewable energy sources in the model area were estimated (see section 2.3).

The goal of this research is to identify a feasible heat production system for a sub-urban region which assures an optimal use of local resources and adapts to the local potentials. The developed methodology during this research enables the local municipality to gain information about possible future heat supply solutions.

2. Energy System Optimisation

The methodology of the optimisation of the energy system is primarily an economic optimisation of a heat supply system using the newly developed framework. Furthermore, the potentials of local energy sources and the heat demand of the building stock were estimated. The following sections give an overview of the methodology used to define the energy system, implement its boundaries, estimate the annual heat demand and the local energy source potentials.

2.1. Energy system definition and optimisation

The heat supply simulation and energy system optimisation are conducted using the developed methodology based on *oemof* [10] and *oemof.solph* [15] shown in Figure 1. With its functionalities and libraries, an energy system model based on user inputs is defined and translated into a linear system of equations using *oemof.solph*. For optimisation of the system, a minimisation problem is defined and solved using open source solving algorithms *pyomo* [17], [18] and *cbc* [19].

As shown on the left in Figure 1 the optimisation is based on various input data which is estimated or calculated (see section 2.2 and 2.3). To define the components of the energy system and most of the necessary input data in this methodology an excel file can be used. Some currently existing functionalities of the existing *oemof*

packages were adapted and further developed. As shown in Figure 1 necessary input data are:

- heat demand profile(s)
- possible energy conversion units (e.g. boilers, CHP units)
- annual CO₂-emission restrictions, funding program restrictions
- timeseries of ambient temperature and variable unit efficiencies
- time series of fluctuating renewable energy sources
- total annual potentials of energy sources (see Table 6)
- economic data (variable and fixed costs (see Table 8, Table 9))

The *oemof.solph* package within the optimisation framework creates a model of the energy system, which is made up of energy sources, sinks, storages, and transformation units. Each transformation unit in this system is represented by a component. The components of the system are connected via buses. A bus is a mathematical connector which can connect several components to represent energy or mass exchange.

A schematic and simplified energy system model for the model region is given in Figure 2. In this schematic overview the main components of the energy system are shown. Energy sources (on the left, e.g. biomass (BM), ambient heat sources and PV) transmit energy flows (represented by arrows) to various transformation units. These so-called transformers convert energy flows from sources into usable energy flows which feed the sinks.

In this study five different transformation units have been considered: CHP, boiler, HP, power to heat (e.g. electrode boiler) (P2H), and storages. A Boiler for natural gas (NG) is considered as condensing boiler. A BM boiler is considered as conventional boiler with lower efficiency than a NG boiler. Transformation units convert several sources of energy to heat and/or electricity.

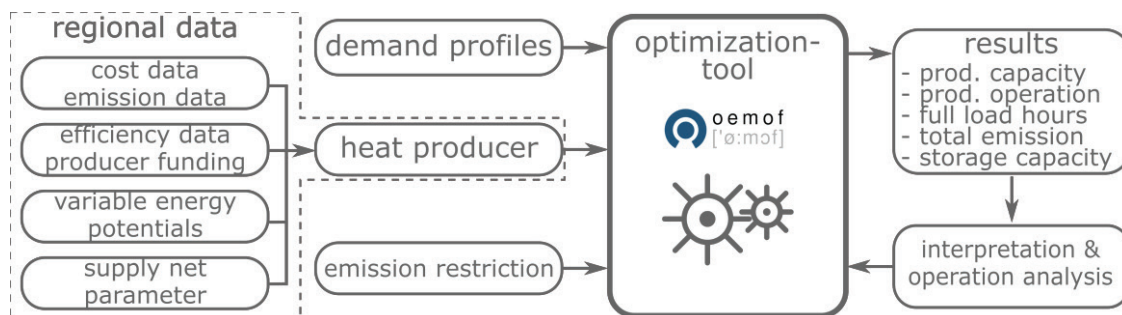


Figure 1: Framework of the optimisation process

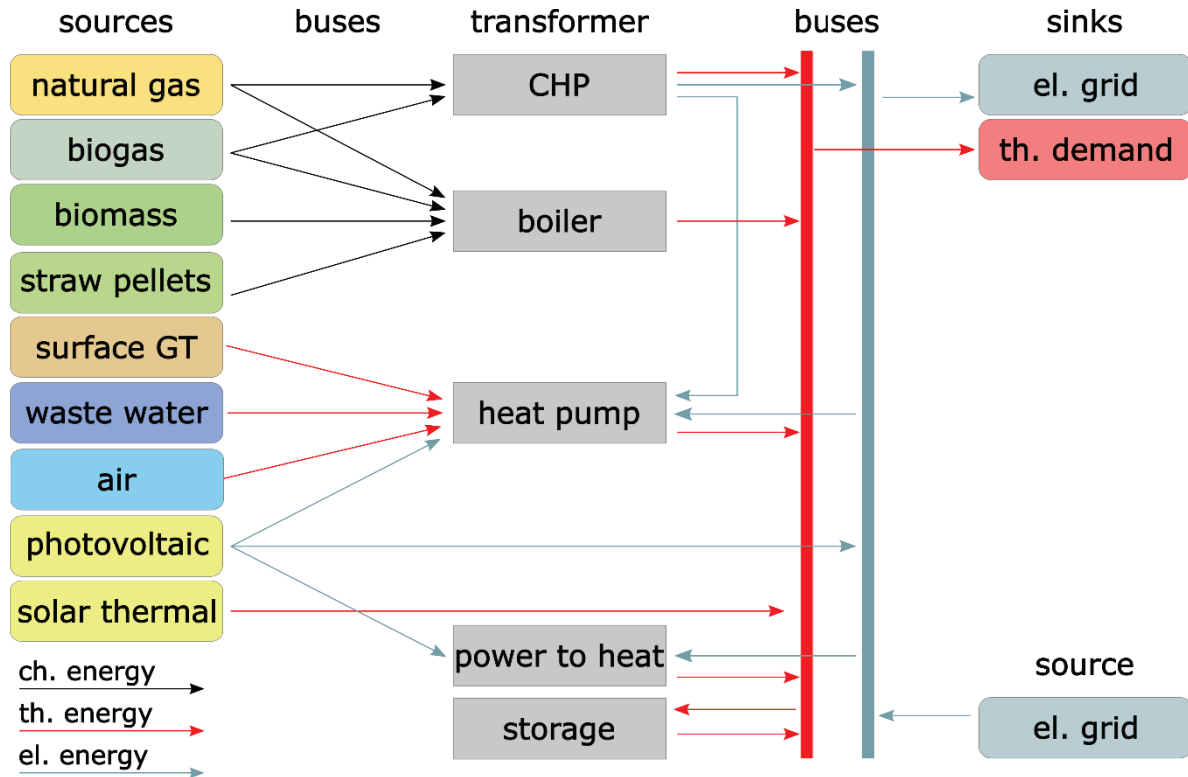


Figure 2: Schematic and simplified overview of the energy system

Storages can store produced surplus energy and discharge it to the grid when needed. For the model region only TES (hot water tanks) are considered as they are cheaper, more efficient, and increase the flexibility the CHP production [20]. Sinks, the thermal and electric grid in the system for example, are shown on the right. The electrical sink in this system represents the local grid for feed in of surplus electricity production. Further it can be used as source for electricity supply of HP or P2H units. Since the electricity supply has so far been provided via an established distribution network, the electricity demand of the households is not taken into account in the design of the heat supply system.

As conventional heat producing units, CHP units and condensing boilers using NG are considered. Solar thermal collectors, several HP systems, or P2H units in combination with PV collectors are considered as renewable heat producing units.

The efficiencies of the transformation units listed in Table 1 are assumed constant over time and independent of the unit size, except those for CHP units. Their efficiencies are constant over time but dependent on the unit's capacity (cap). The efficiency ranges for a small CHP unit (10 kW) from thermal/electrical efficiencies of

0.55/0.35 to efficiencies of 0.45/0.42 for a unit with a capacity of 2,000 kW. Part load efficiencies or start-up phenomena of these units during operation are not considered.

For each of these components (sources, transformers, storages, and sinks) an integral energy balance equation considering a closed system is defined. The balance equation is discretised according to the timestep. In this study, a time step resolution of one hour is chosen, as recommended in [2], among others. The entire energy system is defined by a linear system of equations (Eq. (1)).

$$\left(\frac{dU}{dt}\right) = \sum \dot{E}_m(t) + \sum \dot{E}_{out}(t) \pm \dot{C}(t) \quad (1)$$

In Eq. (1) U represents the internal energy of a component for each timestep t . \dot{E} represent energy flows to and from a component. \dot{C} represents energy conversion or losses inside a component at each timestep, e.g. heat losses of a TES. For each timestep a minimisation problem is solved using functionalities of *oemof.solph* [15]. The objective function of the optimisation Eq. (2) is the minimisation of total annual levelised costs of the

Table 1: Constant efficiency ranges of transformer units

Producer	Size range	Unit	Efficiency range [-]	
			thermal	electrical
CHP	10–2,000	kW _{th}	[0.55; 0.45]	[0.35; 0.42]
Condensing boiler	50–2,000	kW _{th}	0.97	
BM boiler	500–2,000	kW _{th}	0.85	
P2H	50–1,000	kW _{th}	0.99	
PV	5–750	kW _{p,el}		0.18

system (AC) with respect to system boundary conditions. Boundary conditions are satisfying the total heat demand Q_{tot} in each timestep (Eq. (3)) without exceeding the given limit of annual CO₂-emission E_{tot} (Eq. (4)). Where c_f represents the specific cost of each energy flow q_f , I_i the specific investment cost regarding the maximum capacity $q_{i,out,max}$ of a component and e_f the specific CO₂-emission of an energy flow.

$$\min_i AC = \sum_{f,t} c_f \cdot q_f(t) + \sum_i I_i \cdot q_{i,out,max} \quad (2)$$

$$s.t. \sum_i q_{i,out}(t) = Q_{demand}(t) \quad \forall t \in [1; 8760] \quad (3)$$

$$s.t. \sum_{f,t} q_f(t) \cdot e_f \leq E_{tot} \quad (4)$$

The economic optimum after minimising the total cost of the system is based on annuities of investment costs and annuities of variable costs. Annuities levelise the cost of initial investments and possible later re-investments over an economic time horizon considering annual cost escalation rates and interest. Various heat producing technologies within capacity ranges (summarised in Table 8) are selected for the model region based on the potential analysis (see section 2.3) and the common technologies available on the market. Annuities of producer costs are adapted to the nominal size of each

producer. Annuities of variable costs are levelised costs considering annual cost escalation rates and interest of fuel costs for example (Table 7).

After the optimisation process and the post-processing of the results, information about optimal investment of producer capacities, the resulting producer operation, annual CO₂-emission of the system, levelised costs of energy production (LCOE) as well as necessary storage capacities is obtained.

2.1.1. CHP unit, boiler, and P2H unit

In Figure 3 the representing model of a transformation unit (in this case a CHP unit) and its nodes is given. Busses in this model are mathematical connectors which connect various system components, the fuel source on the left and the CHP for example. Through a bus no flow conversion takes place.

Using the defined thermal and electrical efficiencies of the CHP unit (see Table 1) the source energy flow is converted into 2 product flows. Each transformation unit (i) and their connections between input and output energy flows are modelled for each timestep using Eq. (5). The efficiencies for the transformer types summarised in Table 1 are set to be constant over time.

$$\sum_{j=1}^m q_{i,out,j}(t) = \sum_{l=1}^{k,m} (q_{i,in,l}(t) \cdot \eta_{i,lj}) \quad (5)$$

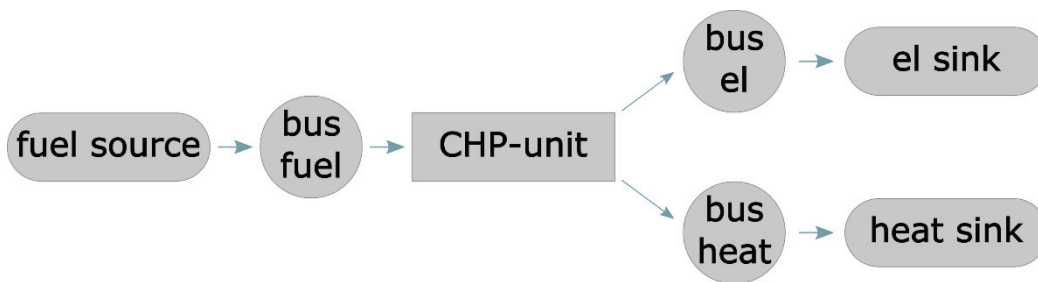


Figure 3: Schematic model of a CHP transformation unit

In Eq. (5) m represents the number of output flows, k represents the number of input flows. In this case two output flows ($m = 2$), an electrical ($j = 1$), and a thermal flow ($j = 2$) are produced from one input flow ($k = 1$). For each output flow of the unit i an efficiency $\eta_{i,j}$ is defined. Similar to the CHP unit a boiler or P2H unit is modelled, e.g. an electrode boiler. Instead of two output flows, only one output and input flow ($k = 1, k = 1$) and one efficiency for energy conversion are defined.

2.1.2. HP unit

For HP units, time dependent instead of constant efficiencies were chosen as they are highly dependent on condensation and evaporation temperature. The condensation temperature is related to the supply temperature of the connected heating grid, which itself is connected to the ambient temperature. The ambient temperature of the test reference year (TRY) 2015 in Germany is used for further calculations. To calculate the coefficient of performance (COP) of HP units the efficiencies according to [21] are used and summarised in Table 2.

The supply temperature of the district heating grid varies between 95°C and 65°C with respect to the ambient temperature. The maximum grid temperature is caused by the highest supply temperature of the oldest buildings present in the model area, whereas the minimum grid temperature depends on the temperature requirements of the domestic hot water (DHW) supply. The maximum possible COP of a compression HP (Eq. (6)) is calculated based on the efficiency of the Carnot cycle [22]. The lower temperature level ($T_{low}(t)$) is calculated using the source temperature ($T_{source}(t)$) and the heat exchanger temperature difference (ΔT_{HE}). Accordingly, the high temperature level ($T_{high}(t)$) is calculated using the sink temperature ($T_{sink}(t)$). For each time step of the optimisation the Carnot efficiency $\eta_{Carnot}(t)$ (Eq. (6)) and the cop of the HP $COP_{HP}(t)$ are calculated (Eq. (7)). Considering a plate heat exchanger for the HP, the temperature difference at the heat exchanger sides is set to $\Delta T_{HE} = 2 K$.

$$COP_{Carnot}(t) = \frac{1}{\eta_{Carnot}(t)} = \frac{1}{1 - \frac{T_{low}(t)}{T_{high}(t)}} \quad (6)$$

$$COP_{HP}(t) = \eta_{HP} \cdot COP_{Carnot}(t) = \frac{\eta_{HP}}{1 - \frac{T_{source}(t) - \Delta T_{HE}}{T_{sink}(t) + \Delta T_{HE}}} \quad (7)$$

The resulting COP of the available heat sources air, wastewater (WW), and surface geothermal (GT) for each time step are shown in Figure 4. Due to fluctuating supply temperatures as well as fluctuating source temperatures, the COP of each technology shows a strong variation on an hourly basis. The COP for air-HP shows a high fluctuation over the whole year due to hourly ambient temperature fluctuations. The COP for WW HP shows high fluctuation during winter months due to supply temperature fluctuation. It is almost constant during summer months due to a constant WW and supply grid temperatures [23]. According to the information provided by the local WW disposal company, the annual WW temperatures range between 12-14°C.

Information on the temperature of surface GT systems is taken from [24]. The COP also shows more fluctuation during winter months than during summer months. There, a steadier curve progression is observed, due to a constant supply temperature and a steady rise of the surface temperature. During September the COP of the surface GT collectors shows a gap at the beginning of the heating period. This is based on the assumption of a higher extraction rate at this point [24]. In case of an unlimited low-temperature heat source, e.g. ambient air, the definition of one conversion factor for electricity is sufficient. To be able to consider limited heat source potentials, e.g. extractable heat from WW, it is necessary to follow the oemof.solph documentation [15] on page 13 to define efficiencies for the conversion of electricity

Table 2: Ambient parameters, supply net parameters and HP efficiencies

Parameter	Unit	Value	Parameter	Unit	Value
Max. supply temp.	°C	95	HP efficiency air/water	-	0.40
Min. supply temp.	°C	65	HP efficiency brine/water	-	0.55
DHW temp.	°C	60	HP efficiency water/water	-	0.55
Min. ambient temp.	°C	-12	Heating surface exponent	-	1.3

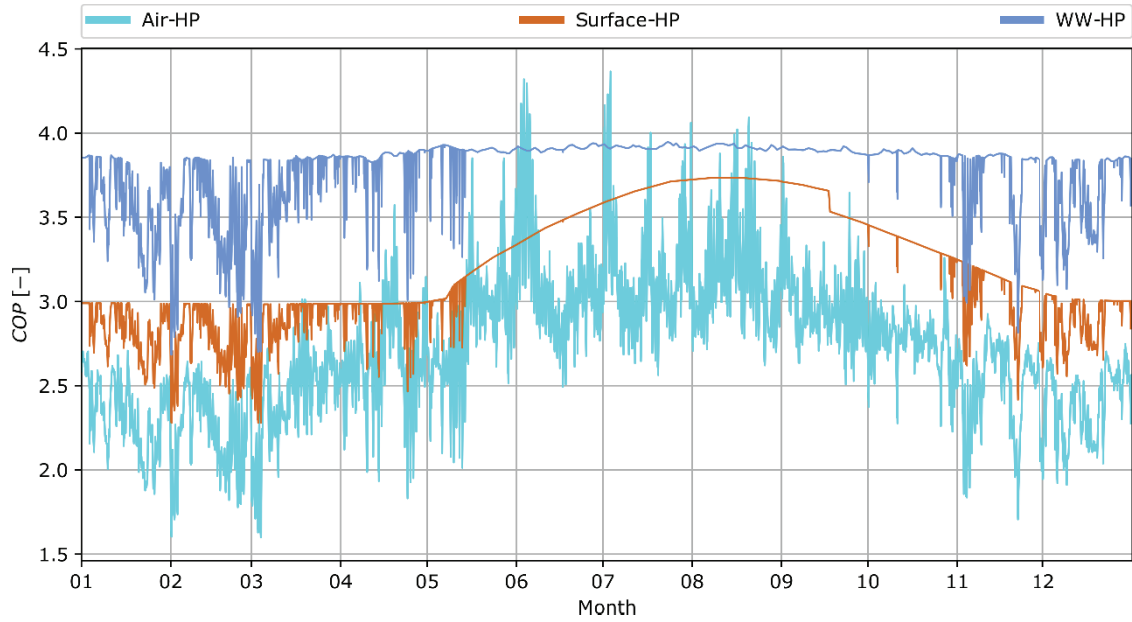


Figure 4: Annual COPs of different HP systems

and the conversion of heat from the heat source (Eqs. (8), (9)). The heat output is calculated using the COP of each timestep (Eq. (10)).

$$\eta_{el}(t) = \frac{P_{el}(t)}{Q_{sink}(t)} = \frac{1}{COP_{HP}(t)} \quad (8)$$

$$\eta_{th}(t) = \frac{Q_{source}(t)}{Q_{sink}(t)} = \frac{COP_{HP}(t) - 1}{COP_{HP}(t)} \quad (9)$$

$$Q_{sink}(t) = P_{el}(t) \cdot \eta_{el}(t) + Q_{source}(t) \cdot \eta_{th}(t) \quad (10)$$

To be able to consider all the different electricity sources of the HP system, a system model as shown in Figure 5 is defined. As input flows, various sources of electricity and heat are possible. The electricity supply of HP can be realised by direct grid supply, self-consumption of the

PV collectors as well as self-consumption of the CHP units. The fluctuation of electricity from renewable energy sources and its specific funding revenues need to be considered to economically optimise the operation of the affected units. The different costs of electricity regarding their production units make a detailed view on HP units and P2H units and its electricity sources necessary (see section 2.1.3).

2.1.3 Auxiliary power system

Due to federal funding restrictions the revenues of electricity generated by CHP or PV units differ depending on the installed capacity of a unit and its annual production. The electricity produced by a CHP unit receives federal funding, as laid out in the Combined Heat and Power Law (Kraft-Wärme-Kopplungs-Gesetz) (KWKG) [25], where the maximum duration of this funding is

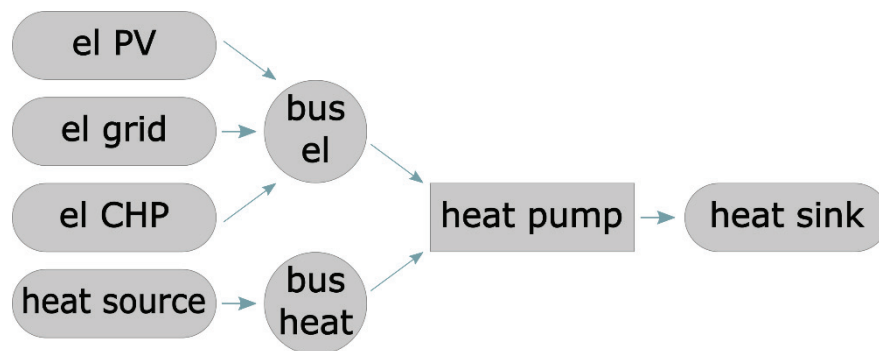


Figure 5: Schematic model of a HP transformation unit

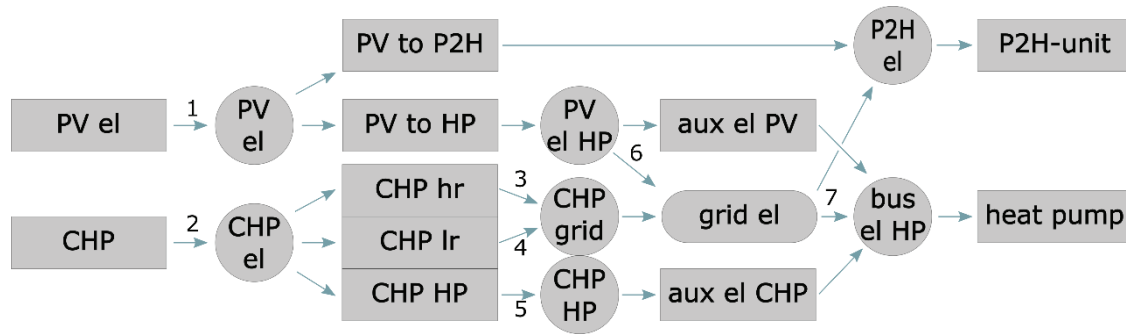


Figure 6: Auxiliary system model for HP electricity supply

also specified. The Renewable Energy Sources Act (Erneuerbare-Energien-Gesetz) (EEG) [26] defines additional costs for self-consumption of electricity from renewable energy sources or CHP units (EEG levy).

For the electricity supply of HP systems, a more complex model with additional auxiliary (aux) transformers and buses was designed to consider all necessary cost and funding flows for accounting and optimisation. In Figure 6 the auxiliary power system for electricity flows from PV units and CHP units is shown. The calculated cost data are summarised in Table 3.

Table 3: Calculated levelised cost of electricity flows in HP systems based on [25], [26]

Flow	Cost description	Range of levelized cost [€/kWh]
1	EEG-levy on CHP and PV electricity production	0.026
2	CHP unit operational cost (excl. fuel cost)	[0.004; 0.020]
3	CHP grid feed in (high revenue)	[-0.121; -0.087]
4	Regular electricity revenue	-0.041
5	Own power consumption cost (incl. EEG-levy)	[-0.009; 0.008]
6	PV grid feed in revenue (refund of EEG-levy)	[-0.125; -0.082]
7	Grid electricity cost for HP systems	0.227

Electricity is produced in the transformation units “PV el”, which represents the PV collector, and the CHP units in the system which convert NG to electricity and heat. For electricity accounting, the heat produced by the CHP unit is not considered in this aux power system.

The produced electricity (with production costs 1, 2) flows to aux transformers (“PV to P2H”, “PV to HP”, “CHP hr”, “CHP lr”, “CHP HP”). For these transformers, efficiency values of 1 are implemented as no flow conversion takes place. The high revenue (hr) electricity

feed-in to the grid of CHP units, which can be achieved for the funding duration, is represented by “CHP hr”. “CHP lr” represents the grid feed-in with low revenue (lr), the common electricity revenue. The electricity produced by PV can be fed into the HP supply transformer (“PV to HP”) and the P2H supply transformer (“PV to P2H”) without additional revenues or costs. From “PV to HP” it can be fed into the local grid with costs 6, or self-consumed in the HP. The revenue for electricity from the CHP units depends on unit size, full load hours (FLH), as well as the fuel source [25].

A limited amount can be fed into the local grid with hr (cost 3) or into the HP system for self-consumption (cost 5). After reaching this limit the grid feed in with lr is possible (cost 4). Without electricity production of both the CHP unit and PV unit the electricity supply of the HP can be realised by consuming electricity from the local grid (cost 7). The supply of the P2H unit with electricity produced in the CHP unit is not considered as the minimum COP for all HP systems (see Figure 4) is higher than the efficiency of the P2H unit. Depending on the electricity source, its cost, and the COP of the HP system the LCOE of the HP varies.

The constraint (Eq. (11)) was implemented limiting the annual amount of electricity which can be funded. As the economic optimisation includes an invest optimisation of the producer size (see Eq. (2)), the CHP capacity of the component is a variable of the optimisation problem. This affects the amount of produced electricity which is applicable for funding (Eq. (12)).

$$\sum_{t=1}^{8760} (q_{CHP,hr}^{el}(t) + q_{CHP,hp}^{el}(t)) \leq FLH_{CHP}^{hr} \cdot q_{CHP,max}^{el} \quad (11)$$

$$FLH_i = \frac{\sum_i q_i^{el}(t)}{q_{i,max}^{el}} \quad (12)$$

$$FLH_{CHP,NG}^{hr} = 3,000 \text{ h/a} \quad (13)$$

$$FLH_{CHP,BG}^{hr} = 4,380 \text{ h/a} \quad (14)$$

For NG units an amount of 30,000 h over 10 years is considered (Eq. (13)) [25]. For CHP units using biogas (BG), 50% of the annual electricity production is compensated with high revenue values (Eq. (14))[26]. If the electricity transport through the transformers “CHP hr” and “CHP HP” exceeds this limit, the energy flow from bus “CHP el” can only be transported through transformer “CHP lr”.

2.1.3. 4th Generation network funding

To consider the federal funding program for 4GDH networks the total amount of heat produced during a year needs to be allocated to its production unit based on the type of heat. Three categories of heat are defined depending on the fuel of the heat producing unit [27]:

- Renewable (index *ren*)
- Biomass (index *bm*)
- Conventional / fossil (index *conv*)

These attributes were added to the flows in the energy system. To apply for the funding program several terms and conditions must be met. The sum of all flows with these attributes (Eqs. (15)-(17)) is taken into account to implement the constraint (Eq. (20)).

$$Q_{ren} = \sum_{t=1}^{8760} q_{ren}(t) \quad (15)$$

$$Q_{bm} = \sum_{t=1}^{8760} q_{bm}(t) \quad (16)$$

$$Q_{conv} = \sum_{t=1}^{8760} q_{conv}(t) \quad (17)$$

At least 50% of the annual heat production must be realised by renewable energy sources according to the funding program [27]. Heat produced from BM can be considered as renewable up to the total amount of all other renewable heat in the system (Eq. (18)). If more heat from BM than from renewable sources is produced, the surplus BM heat is considered as conventional/fossil heat (Eq. (19)).

$$Q_{bm,ren} = \begin{cases} Q_{bm} & Q_{bm} \leq Q_{ren} \\ Q_{ren} & Q_{bm} > Q_{ren} \end{cases} \quad (18)$$

$$Q_{bm,conv} = Q_{bm} - Q_{bm,ren} \quad (19)$$

$$Q_{ren} + Q_{bm,ren} \geq Q_{conv} + Q_{bm,conv} \quad (20)$$

A higher share of renewable heat in the systems offers the possibility to receive more funding awards [28]. A constraint to specify the desired additional percentage share (*R*) of renewable heat in the energy system based on the EEG [28] is implemented (see Eq. (22)). A factor of 8 for example means an additional share of 40% of annual renewable heat production of the system in addition to the minimum of 50%.

$$Q_R = Q_{ren} + Q_{bm,ren}, \quad Q_C = Q_{conv} + Q_{bm,conv} \quad (21)$$

$$Q_R \cdot 100 \geq (Q_R + Q_C) \quad (22)$$

$$\cdot \left(\left(\frac{R}{10} \right) \cdot (Q_{R,max} - Q_{R,min}) + Q_{R,min} \right)$$

$$Q_{R,max} = 100, \quad Q_{R,min} = 50 \quad (23)$$

2.2. Model region specifics and demand profile simulation

The model area consists of a heterogeneous building stock of 217 buildings of which 58% are residential and 42% are non-residential buildings. Most buildings, with regard to the net heated area, are constructed before 1984 (64.2%). The building parameters, such as building type, year of construction, and renovation status vary over the model area. The categories of the construction year of buildings of the model area are summarised in Table 4.

Table 4: Building age categories of model area

Year of construction	Quantity	Quantity [%]	Area [m ²]	Area [%]
before 1948	37	15.2	19,009	13.9
1949-68	24	9.9	9,869	7.2
1969-83	55	22.6	58,922	43.1
1984-2010	38	15.6	26,795	19.6
after 2010	63	36.6	22,257	16.3

A school complex of three buildings, a new constructed supermarket, and buildings with mixed commercial and living usages are the main representatives of non-residential buildings. To simulate the heat load of the model region a detailed study of the building stock was conducted, where inquiries with habitants and database analysis of building parameters were combined. Building models were automatically generated and simulated using the tool Teaser [29]. Separate load profiles for

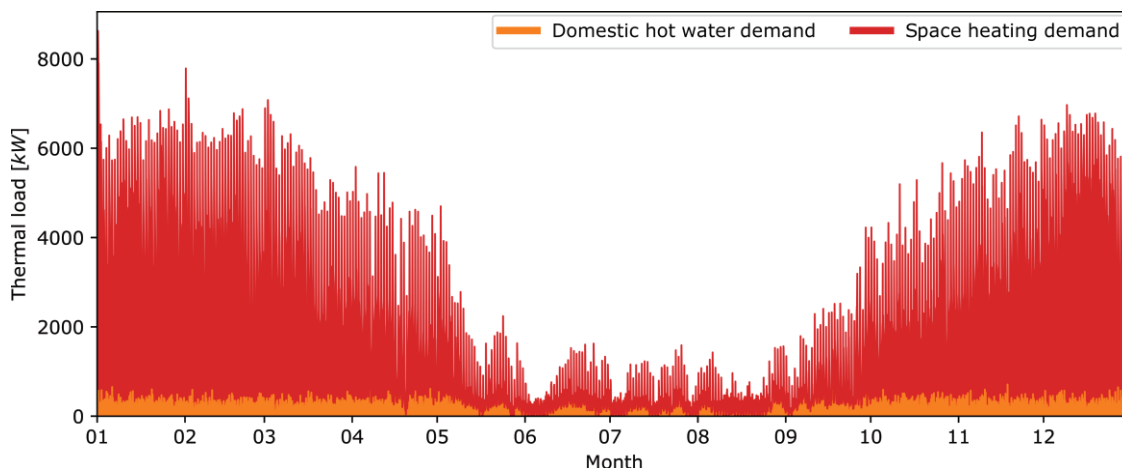


Figure 7: Hourly heat demand profiles of the model region

domestic hot water and space heating were created. Due to a cooling demand only in the supermarket, which is planned as self-sufficient including waste heat utilisation, the design of a district cooling network is not considered.

Load profiles of domestic hot water were created by scaling nominal domestic hot water profiles according to each building’s net leased area. Load profiles for space heating were created by scaling individual reference building load profiles based on the residential buildings of the German building typology Tabula [30]. Data such as the respective building’s net leased area, partial renovations of windows, facade, roof, and floor were included in the scaling. As a result, load profiles from the corresponding building’s space heating and domestic hot water demand were generated for the complete model area using a timestep of an hour (see Figure 7).

Table 5: Current heat producing units and percentage share of annual heat production

Heat producer unit	Number of units	Share of annual heat production [%]
Boiler (oil)	27	5.7
Boiler (NG)	212	72.5
HP	15	3.0
CHP, boiler (NG, school complex)	3	18.8

The average hot water demand is almost constant throughout the year, except for the period from May to September. In comparison, the space heating demand shows a high fluctuation, which is quite common for heat supply networks and a heterogeneous building stock [31]. The highest demand occurs in the months from November to April. In the summer months, the demand for space heating is correspondingly low. The

simulated annual heat demand is 16,524 MWh_{th}/a with a thermal peak load of approx. 8,600 kW_{th}.

The current state heat production is realised independently for each building mainly depending on NG and oil. In Table 5 the currently installed heat producing units and their percentage share of annual heat production are shown. The total annual CO₂-emission of the existing energy system is approx. 3,852 t/a. The LCOE in €-cent (ct) per kWh_{th} of the current energy system is approx. 11.2 ct/kWh_{th}. These data represent the reference case for later comparisons.

2.2. Model region energy potentials and economic parameters

In order to apply the developed methodology to a specific case study, local energy potentials were estimated. The available renewable energy sources in the model region and their estimated potentials are summarised in Table 6.

Table 6: Theoretical potentials of renewable energy sources

Source	Potential in GWh/a	Source	Potential in GWh/a
WW-HP	2.1	Wood chips (local)	6.0
GT-collector	17.2	Straw pellets	19.5
GT-probes	19.1	PV	1.2

Local companies as e.g. a municipal waste disposal company, provided information on the energy potentials of WW and BM within the model area. Further energy potentials using different ambient heat sources, e.g. surface GT collectors or probes in combination with HP, were considered estimating good temperature levels and stability [32]. The data of the average daily WW volume of 2400 m³/d and a cooling of 2 K results in an annual potential of approx. 2.1 GWh_{th}/a.

In regional proximity (≤ 50 km), different sources of BM such as wooden BM and straw pellets are available. A municipal waste disposal company could provide woodchips with an energetic potential of approx. 6 GWh_{th}/a (wood chips (local)). The purchase of additional wood chips or wood pellets at market conditions is considered as well (wood chips (market), wood pellets).

Due to renaturation programs of swamps and moors in the area, the usage of straw pellets as BM source can also be considered and its potential was estimated to 19.5 GWh_{th}/a. However, the first analyses of this energy source showed that its production and transportation cost will be higher compared to other BM sources. The potential of GT-collectors (17.2 GWh_{th}/a) and GT-probes (19.1 GWh_{th}/a) was calculated according to [33], [34] for surface collectors with a depth (≤ 5 m) and probes with a possible depth of (≤ 100 m). For the potential analysis, the available net area, which includes all undeveloped surfaces, was used. These technologies are in direct competition with each other through the use of the same area. Suitable roof areas in terms of orientation and inclination (3.7 ha) of the total roof areas (7.2 ha) within the model region could be used for the installation of PV or solar thermal collectors. Due to different

ownership structures and uncertainties about the actual usable roof areas, only roof areas of public buildings were considered. These roof areas could situate approx. 6,100 m² collector surface. Using the data of [35] and assuming a southerly orientation and an inclination of 30° of PV collectors, this results in an annual potential of 1.2 GWh_{el}/a.

Theoretically, the annual heat production potential of all renewable energy sources can meet the annual heat demand of the model region. Realistically, the fluctuation of the heat demand and renewable energy sources over the year and even over one day must be considered.

NG is considered as a possible fossil energy carrier. The use of BG is considered on a balance sheet basis because no BG plant is situated in direct surrounding of the model area. The local electricity grid is considered as a source of electricity. Depending on the supply contract and the amount of annual electricity demand e.g. for residential or commercial customers, the costs for electricity can vary. For usage in sector coupling systems such as electrode boilers (P2H) or HP systems different prices are implemented. Economic parameters, e.g. cost escalation rates (see Table 7), were used to calculate the specific investment costs ranges of the considered heat producing units (see Table 8), as well

Table 7: Cost elevation rates and calculated economic parameters [36], [37]

Parameter	Unit	Value	Parameter	Unit	Value
NG	% p.a.	2.45	BG	% p.a.	2.45
BM	% p.a.	0.72	Electricity	% p.a.	0.74
CO ₂ -cost	% p.a.	2.00	Maintenance cost	% p.a.	2.45
Invest cost	% p.a.	0.60	Other cost	% p.a.	0.60
Economic horizon	a	20	Annuity factor	-	0.076

Table 8: Levelised specific investment cost of producing units adapted from [36], [37]

Producer	Size range	Unit	Levelized invest cost	Unit
CHP	10–2,000	kW _{el}	475.9–81.5	€/kW _{el} /a
Condensing boiler	50–2,000	kW _{th}	18.7–6.7	€/kW _{th} /a
Biomass boiler	500–2,000	kW _{th}	80.4	€/kW _{th} /a
Air-HP	10–2,000	kW _{th}	90.4–40.7	€/kW _{th} /a
GT-probe-HP	10–200	kW _{th}	187.2–142.8	€/kW _{th} /a
GT-collector-HP	10–200	kW _{th}	138.6–110.5	€/kW _{th} /a
WW-HP	100–500	kW _{th}	114.4	€/kW _{th} /a
P2H	50–1,000	kW _{th}	19.5–17.8	€/kW _{th} /a
TES	10-20,000	kWh _{th}	1.183	€/kWh _{th} /a
PV	5–750	kW _{p,el}	152.8–73.3	€/kW _{p,el} /a

Table 9: Specific cost and specific CO₂-emission of energy carrier adapted from [36], [37]

Energy carrier	Levelized cost [€/kWh]	Specific CO ₂ -emission [kg/kWh]
NG	0.0387	0.240
BG	0.0982	0.120
Wood chips (local)	0.0127	0.026
Wood chips (market)	0.0343	0.026
Wood pellets	0.0525	0.029
Straw pellets	0.0579	0.040
Electricity (residential)	0.3233	0.340
Electricity (commercial)	0.1796	0.340
Electricity (P2H)	0.1169	0.340
Electricity (HP)	0.2266	0.340

as the levelised costs of considered energy carriers (see Table 9).

The specific CO₂-emission of considered energy carriers are also given in Table 9. The levelised cost for CO₂-emission is 62 €/t based on current decisions of the federal government.

3. Main Results

To support the local administration in deciding on an optimal solution for the municipality’s future heat supply system, several scenarios were defined during the project. A variety of CO₂-emission reduction scenarios, as well as scenarios with preferred system parameters, such as annual share of renewable heat, have been investigated. For this article and in the context of Smart Energy Systems-4th Generation District Heating, the most relevant design scenarios were chosen. Their main optimisation parameters are listed in Table 10.

The first design scenario (a) is a static design method using an ordered annual load curve to estimate unit capacities for the most economic annual heat production. In the second and third design scenario (b, c), the developed methodology is applied. Additional constraints are implemented in order to fulfil requirements of the federal funding program or annual CO₂-emission reduction (red) goals. Scenario b is called the 4th generation scenario, where a constraint was set to assure an

annual renewable heat production of 90%. In the third scenario (c) a high level of CO₂-emission reduction (80% compared to the reference case) was defined as a constraint. This scenario is called the 80%reduction scenario.

3.1. Static design approach

A static design method was chosen as the first design approach. An ordered annual load curve of the load profile was used, and heat producer sizes were designed based on ideal FLH (see Figure 8). The base load due to the lowest heat production cost is realised by a BM boiler. It is supplied by locally available wood chips without additional purchase of market wood chips. The mid and peak loads are produced by a NG condensing boiler. The heat production fits the heat demand exactly, as it is one of the design requirements. Heat storage is not considered in this scenario.

With the static design approach, the economically optimal heat producing solution was calculated without consideration of fluctuating sources, CO₂-emission constraints, storage management or time dependent cop of HP. This method of energy system design leads to a non-satisfying solution. The estimated results of approx. 2,951 t/a annual CO₂-emission which compared to the reference case represents a reduction of 23.4%. A BM boiler with wood chips from a local supplier as well as a

Table 10: Main parameters of the optimisation

Parameter	Unit	Value	Main scenarios	Unit	Value
Annual heat demand	GWh	16.8	(a) Static design	-	-
Max. heat load	MW	8.7	(b) Renewable share	%	90
Current emissions	t/a	3,852	(c) Emission reduction	%	80

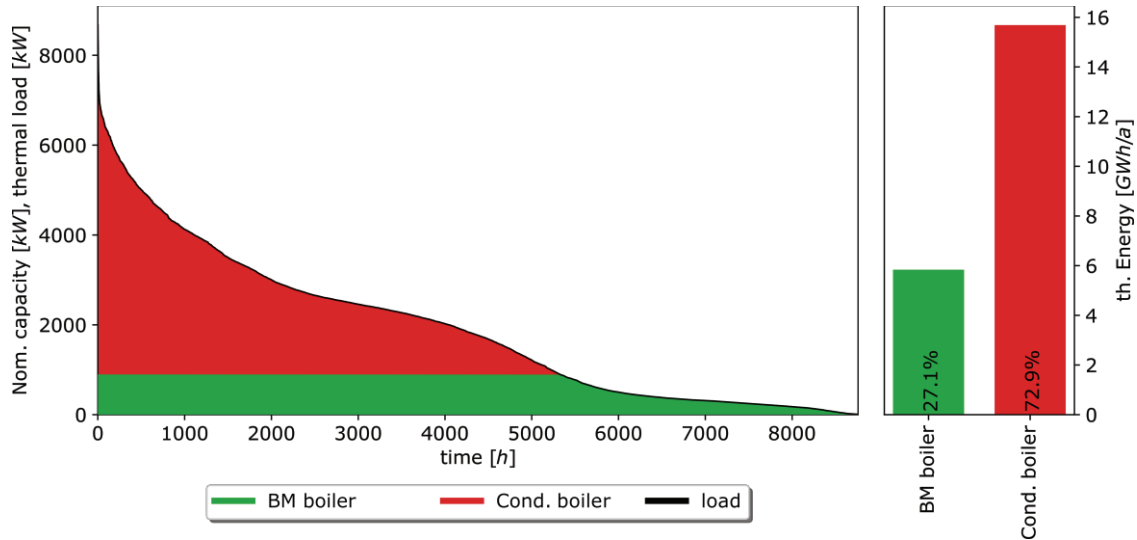


Figure 8: Annual load curve and annual heat share, static design approach

NG boiler are installed. These units have the lowest fuel and investment costs (Table 8, Table 9). This leads to LCOE in €-ct per kWh_{th} of this system of approx. 6.9 ct/kWh_{th} which represents a reduction of 38.1% compared to the reference case. These costs include 2.2 ct/kWh_{th} specific cost of the heat supply grid.

3.2. 4th generation scenario

The optimisation results of the 4th generation scenario using the developed methodology are shown in Figure 9. At first sight, a more diverse energy system can be observed. The base load is satisfied by a WW-HP, a GT-HP, and a CHP unit. The main heat demand is satisfied by a BM boiler. An air-HP, a P2H unit and a NG condensing boiler cover peak load hours. When the heat production exceeds the actual demand, the excess heat is stored in TES. During peak and low load hours the heat demand is not satisfied by the installed units. During these hours heat with lower specific cost and specific CO₂-emission is discharged from the TES instead.

A more detailed view of the annual heat production and the percentage share can be seen on the right. The boundary condition of the system requiring a minimum of 90% renewable heat is satisfied by the HP units, the P2H unit, and the BM boiler. The CHP unit and the condensing boiler together account for 10% of the produced heat.

The total annual CO₂-emission of the optimised energy system is 1,240 t/a which represents a reduction of 67.8% compared to the reference case. The optimised storage size in this scenario is 13.6 MWh_{th}. Due to heat

losses of the supply grid and the heat storage, the total annual heat production is 17,265 MWh_{th}/a. The LCOE are approx. 6.7 ct/kWh_{th}, including 1.5 ct/kWh_{th} specific cost of the supply grid, less than in scenario a due to the funding revenues in this scenario. As this scenario mainly depends on HP systems, information about the electricity supply of these units is presented in Figure 10.

The sum of electricity consumed by all HP systems over one year is shown on the left. On the right, the annual power consumption of each HP system is shown. During the summer months (June till September) the supply can be provided almost completely by the PV unit. At some points during August and October the CHP unit and grid supply are required to cover the higher electricity demand. During the heating period from October to May and during winter months, the electricity produced by PV cannot satisfy the demand for the HP systems and the supply is mainly supplied by the CHP unit. During peak load hours during December till March additional grid supply is necessary. Using the gained information about the optimal operation of the HP systems, the seasonal performance factor (SPF) of the HP systems can be calculated. These are summarised in Table 12.

3.3. 80% Reduction scenario

In Figure 11 the annual load curve of the 80% reduction scenario is shown. The HP systems are partly displaced by a BM boiler with high capacity and a high level of annual FLH. Compared to the 4th generation scenario, the installed capacity has increased by 53% and the

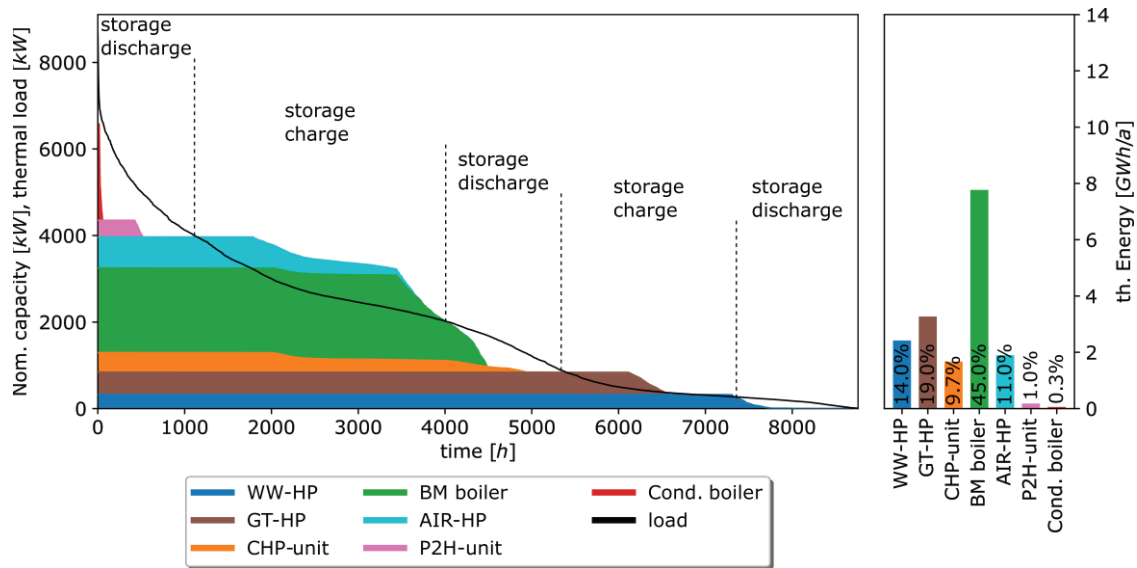


Figure 9: Annual load curve and annual heat share, 4th-generation scenario

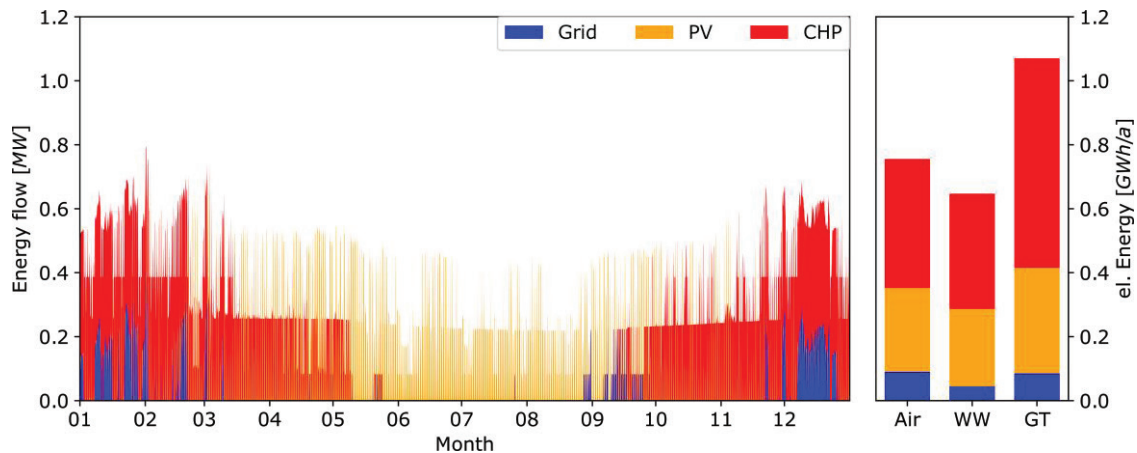


Figure 10: Annual electricity flows to HP systems, 4th-generation scenario

annual share of heat production of this unit has increased from 45% to 78.4%, as shown in Figure 11 on the right. As BM is the energy source with the lowest specific CO₂-emission, this energy system depends mainly upon it. The installed capacity of the air HP system as well as that of the installed capacity of the CHP unit is reduced to a quarter of that found in the 4th generation scenario. The installed capacity of the WW-HP is similar. The FLH and annual share of produced heat of these units have decreased significantly. The total annual CO₂-emission of the system is approx. 771 t/a. According to the restrictions of the federal funding program for renewable heat from BM (see Eq. (11)), a total share of 30% of the annual heat produc-

tion can be considered as renewable heat. As this stands, the required 50% renewable heat production have not been met.

Given that the currently known local thermal potential of wooden BM is approximately 6 GWh_{th}/a, this energy system would be largely dependent on the purchase of BM from the market with an additional thermal potential of 7.3 GWh_{th}/a. During mid load hours, excess heat is stored. This is then discharged during peak and low load hours. The optimised storage size in this scenario is 10 MWh_{th}. The total annual heat production is 16,941 MWh_{th}/a due to decreased heat losses of the heat storage. The LCOE are approx. 7.3 ct/kWh_{th} (including grid cost of 2.2 ct/kWh_{th} without funding). As the BM

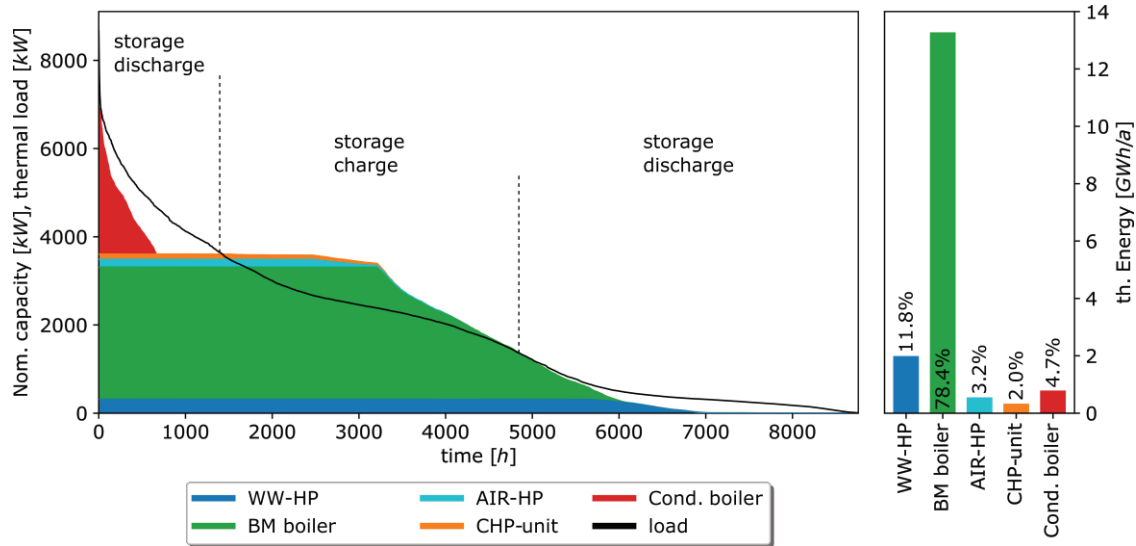


Figure 11: Annual load curve and producer capacities, 80%-reduction scenario

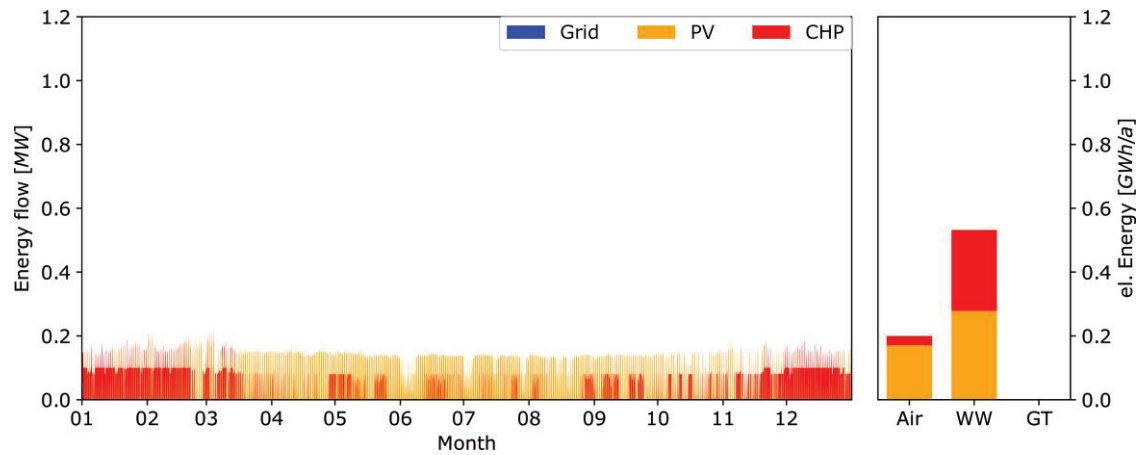


Figure 12: Annual electricity flows to HP systems, 80%-reduction scenario

boiler is the largest producer of heat in this scenario the amount of electricity supply to the HP units is significantly lower. The share of electricity supply for the HP systems in the high reduction scenario is shown in Figure 12.

On the left the sum of electricity consumed by all HP systems over one year is shown; on the right the annual amount of power consumption of each HP system. A surface GT-HP in this scenario is not present due to lower annual cop compared to WW-HP systems (see Figure 4) and significantly higher investment costs than air-HP systems (see Table 8). The electricity supply of the air-HP and WW-HP systems can be provided by the PV unit (61%) and by the CHP unit (39%). The opera-

tion of the CHP unit mainly takes place during the months from November to April but is necessary during the summer months as well. The electricity supply of the local grid is not necessary. The SPF of the HP are summarised in Table 12.

3.4. Results summary

The main results are summarised in Table 11 and a comparison of the three designed energy systems is given in Figure 13.

On the left in Figure 13 the installed capacity of each unit is presented, on the right the annual heat production. Using the static design (left bar) results in higher installed capacities. The installed capacity in both

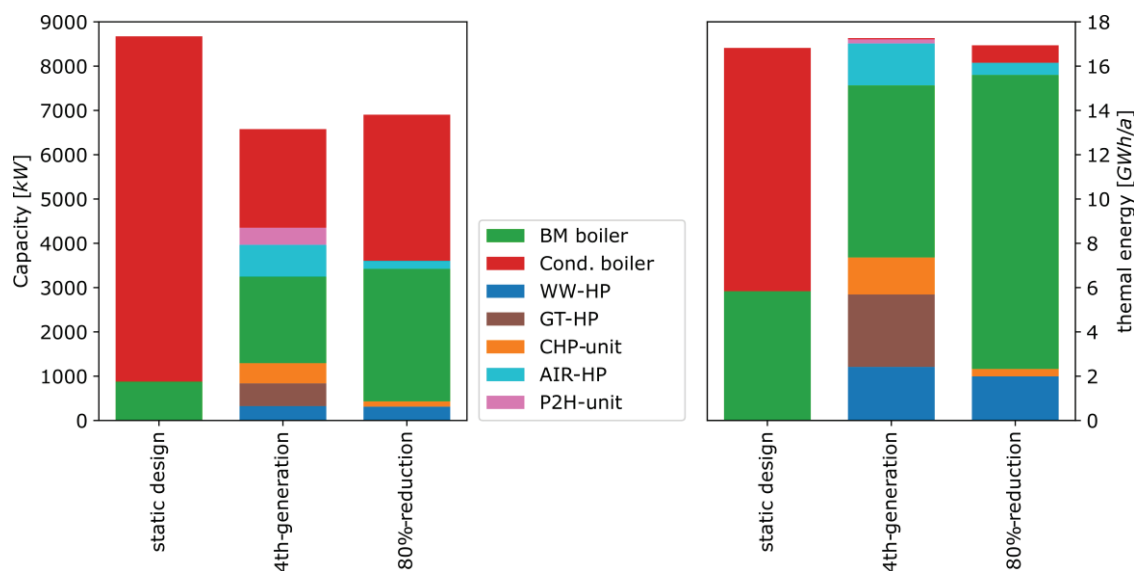


Figure 13: Installed unit capacity and annual heat production of the design scenarios

Table 11: Main results of the current supply system (reference) and the design scenarios

Scenario	LCOE [ct/kWh]	LCOE red. [%]	CO ₂ -emission [t/a]	CO ₂ -emission red. [%]	Installed cap. [kW]
Reference case	11.2	-	3,852	-	n.a.
(a) Static design	6.9	38.1	2,951	23.4	8,673
(b) 4th-generation	6.7	40.2	1,240	67.8	6,578
(c) 80%-reduction	7.3	35.3	771	80.0	6,904

optimised scenarios is significantly lower due to the installation of a heat storage unit. The usage of NG, BM and various renewable energy sources leads to lower annual CO₂-emission when compared to the oil and NG usage in the reference system.

With the optimised operation of the heat producer, further CO₂-emission reduction is possible. Due to the federal funding program, the LCOE of the 4th generation scenario are lowest in this study. The potential of CO₂-emission reductions with comparable LCOE is shown in the 80%-reduction scenario. However, the high share of BM in this scenario makes the system vulnerable to supply shortages and is mainly dependent on local BM production capacities.

Comparing the SPF (Table 12) shows that the more efficient operation of the air-HP takes place in the 80% reduction scenario because the base load is satisfied by the BM boiler with low specific CO₂-emission. The air-HP is only operated when the cop is high and PV electricity is available. The annual performance of the

WW-HP is comparable in both scenarios as it is mainly operated in base load.

Table 12: Seasonal performance factors (SPF) of operated heat pump systems

Scenario	SPF air-HP	SPF	
		WW-HP	GT-HP
(b) 4 th -generation	2.51	3.74	3.06
(c) 80%-reduction	2.76	3.75	-

4. Conclusion

The methodology developed in this study, adapting functionalities of oemof, made it possible to calculate various scenarios for the future energy system of a municipality. It enabled the consideration of the special requirements of two federal funding programs and allowed their definition as additional constraints for the optimisation problem. Based on the optimisation results, economically optimised design solutions which fulfil additional

objectives were developed, especially involving CO₂-emission reduction and desired heat production from renewable sources. The electricity supply of HP systems and the influence of the fluctuating electricity sources on these systems were calculated and interpreted.

The combinations of P2H and HP units with PV and CHP units were given special consideration. It was shown that heat production from these systems, considering fluctuating efficiencies and electricity sources, led to a heat supply system design with a CO₂-emission reduction potential of 67-80% and LCOE of 6.7 ct/kWh_{th} respectively 7.3 ct/kWh_{th}.

Beside all uncertainties of the static design approach a future heating supply network has a potential of reducing annual CO₂-emission by 23% compared to the reference case. The dynamic optimisation of the operation of producing units using the developed methodology show further CO₂-emission and cost reduction potentials. The linearity of the system and its balance equations lead to several uncertainties which are the subject of further investigations in this project. Considering constant part load efficiencies of producing units lead to an underestimation of fuel consumption for some units with decreasing part load efficiencies. Further, the power to heat ratio of CHP units is affected by part load operation, which was not considered. Real operation restrictions like up and down time or start up behaviour of units could not be considered at this time. Frequent non-constant operation of units could lead to higher equipment wear which could negatively affect the working life of said units, resulting in a shortened re-investment cycle and a higher overall LCOE.

For a realistic implementation of the optimised system, it is necessary to control the producer park during operation, considering measurement data. Concepts for implementation are currently being investigated.

5. Acknowledgements

The authors thank the editorial [38] and the organisers of the 6th International Conference on Smart Energy Systems from 6th till 7th October 2020 in Aalborg and online due to the COVID-19 pandemic. Furthermore, the authors thank the Federal Ministry for Economic Affairs and Energy (Bundesministerium für Wirtschaft und Energie) (BMWi) for supporting and funding the project (03ET1597A) on the basis of a decision by the German Bundestag and additionally to the other Suburbane Wärmewende project partners for their support and inspiration.

References

- [1] D. M. Sneum and E. Sandberg, "Economic incentives for flexible district heating in the nordic countries," *Int J Sustain Energy Plan Manag*, vol. 16, pp. 27–44, 2018, <https://doi.org/10.5278/ijsepm.2018.16.3>.
- [2] H. Pieper, V. Mašatin, A. Volkova, T. Ommen, B. Elmegaard, and W. Brix Markussen, "Modelling framework for integration of large-scale heat pumps in district heating using low-temperature heat sources," *Int J Sustain Energy Plan Manag*, vol. 20, 2019, <https://doi.org/10.5278/ijsepm.2019.20.6>.
- [3] H. Lund and J. Z. Thellufsen, "EnergyPLAN - advanced energy systems analysis computer model." Zenodo, 2020, <https://doi.org/10.5281/zenodo.4017214>.
- [4] C. Saletti, M. Morini, and A. Gambarotta, "The status of research and innovation on heating and cooling networks as smart energy systems within horizon 2020," *Energies*, vol. 13, no. 11, p. 2835, 2020, <https://doi.org/10.3390/en13112835>.
- [5] J. Knies, "A spatial approach for future-oriented heat planning in urban areas," *Int J Sustain Energy Plan Manag*, vol. 16, pp. 3–30, 2018, <https://doi.org/10.5278/ijsepm.2018.16.2>.
- [6] V. Heinisch, L. Göransson, M. Odenberger, and F. Johansson, "Interconnection of the electricity and heating sectors to support the energy transition in cities," *Int J Sustain Energy Plan Manag*, vol. 24, 2019, <https://doi.org/10.5278/IJSEPM.3328>.
- [7] P. Lazzeroni, "Design of a polygeneration system with optimal management for a dhc network," *Int J Sustain Energy Plan Manag*, vol. 22, 2019, <https://doi.org/10.5278/IJSEPM.2450>.
- [8] R. van Leeuwen, J. B. de Wit, and G. J. M. Smit, "Energy scheduling model to optimize transition routes towards 100% renewable urban districts," *Int J Sustain Energy Plan Manag*, vol. 13, pp. 19–46, 2017, <https://doi.org/10.5278/ijsepm.2017.13.3>.
- [9] H. Lund, S. Werner, R. Wiltshire, S. Svendsen, J. E. Thorsen, F. Hvelplund, B. V. Mathiesen, "4th generation district heating (4GDH)," *Energy*, vol. 68, pp. 1–11, 2014, <https://doi.org/10.1016/j.energy.2014.02.089>.
- [10] S. Hilpert, C. Kaldemeyer, U. Krien, S. Günther, C. Wingenbach, and G. Plessmann, "The open energy modelling framework (oemof) - a new approach to facilitate open science in energy system modelling," *Energy Strategy Reviews*, vol. 22, pp. 16–25, 2018, <https://doi.org/10.1016/j.esr.2018.07.001>.
- [11] S. Hilpert, S. Günther, C. Kaldemeyer, U. Krien, G. Plessmann, F. Wiese, C. Wingenbach, "Addressing energy system modelling challenges: The contribution of the open energy modelling framework (oemof)," 2017, <https://doi.org/10.20944/preprints201702.0055.v1>.
- [12] Md. N. I. Maruf, "Sector coupling in the north sea region—a review on the energy system modelling perspective," *Energies*,

- vol. 12, no. 22, p. 4298, 2019, <https://doi.org/10.3390/en12224298>.
- [13] C. Möller, K. Kuhnke, M. Reckzügel, H.-J. Pfisterer, and S. Rosenberger, “Energy storage potential in the northern german region Osnabrück-Steinfurt,” in *2016 international energy and sustainability conference (IESC)*, 2016, pp. 1–7, <https://doi.org/10.1109/IESC.2016.7569497>.
- [14] C. Kaldemeyer, C. Boysen, and I. Tuschy, “Compressed air energy storage in the german energy system – status quo & perspectives,” *Energy Procedia*, vol. 99, pp. 298–313, 2016, <https://doi.org/10.1016/j.egypro.2016.10.120>.
- [15] oemof developer group, “oemof.solph Release 0.4.2.dev0 documentation”, 2021, https://oemof-solph.readthedocs.io/_downloads/en/latest/pdf/
- [16] J. A. Bondy and U. S. R. Murty, “Graph theory,” vol. 244. Springer, New York, 2008.
- [17] W. E. Hart et al., *Pyomo - optimization modeling in python*, Second edition., vol. 67. Cham, Switzerland: Springer Science & Business Media, 2017, <https://doi.org/10.1007/978-3-319-58821-6>.
- [18] W. E. Hart, J. P. Watson, and D. L. Woodruff, “Pyomo: Modeling and solving mathematical programs in python,” *Mathematical Programming Computation*, vol. 3, no. 3, pp. 219–260, 2011, <https://doi.org/10.1007/s12532-011-0026-8>.
- [19] J. Forrest et al., “Coin-or/cbc: Version 2.9.9.” Zenodo, 2018, <https://doi.org/10.5281/zenodo.1317566>.
- [20] H. Lund, B. V. Mathiesen, D. Connolly, and P. A. Ostergaard, “Renewable energy systems - a smart energy systems approach to the choice and modelling of 100 % renewable solutions,” *Chemical Engineering Transactions*, vol. 39, pp. 1–6, 2014, <https://doi.org/10.3303/CET1439001>
- [21] oemof developer group, “Oemof-thermal: Thermal energy components in oemof.” Zenodo, 2020, <https://doi.org/10.5281/zenodo.3606385>.
- [22] VDE ETG Energietechnik, “Potenziale für Strom im Wärmemarkt bis 2050 - Wärmeversorgung in flexiblen Energieversorgungssystemen mit hohen Anteilen an erneuerbaren Energien.” VDE ETG Energietechnik, 2015, Accessed: Feb. 04, 2021. [Online]. Available: http://www.energiesdialog2050.de/BASE/DOWNLOADS/VDE_ST_ETG_Warmemarkt_RZ-web.pdf.
- [23] O. Wanner, “Wärmerückgewinnung aus Abwassersystemen.” Bundesamt für Energie (BFE), 2004, Accessed: Feb. 04, 2021. [Online]. Available: https://www.eawag.ch/fileadmin/Domain1/Abteilungen/eng/projekte/abwasser/Waermerueckgewinnung/BFE_Schlussbericht.pdf.
- [24] Bundesindustrieverband Deutschland Haus-, Energie- und Umwelttechnik e.V. (BDH), “Informationsblatt Nr. 43: Auslegung von oberflächennahen Erdwärmekollektoren.” Cologne, 2011, Accessed: Feb. 04, 2021. [Online]. Available: https://www.waermepumpe.de/uploads/tx_bcpagflip/bwp-Infoblatt43-Erdwaermekollektoren.pdf.
- [25] Bundesministerium für Wirtschaft und Energie, “Gesetz für die Erhaltung, die Modernisierung und den Ausbau der Kraft-Wärme-Kopplung (Kraft-Wärme-Kopplungsgesetz - KWKG).” 2017, Accessed: Feb. 04, 2021. [Online]. Available: https://www.bmwi.de/Redaktion/DE/Downloads/Energie/kwkg.pdf?__blob=publicationFile&v=6.
- [26] Bundesministerium für Wirtschaft und Energie, “Gesetz für den Ausbau erneuerbarer Energien (Erneuerbare-Energien-Gesetz - EEG 2017: BGBl. s.1 (1066).” 2017, Accessed: Feb. 04, 2021. [Online]. Available: https://www.bmwi.de/Redaktion/DE/Downloads/E/ee-g-2017-gesetz-en.pdf?__blob=publicationFile&v=8.
- [27] Bundesministerium für Wirtschaft und Energie, “BAnz AT 24.12.2019 B1 - Wärmenetze 4.0 - Bundesförderung effiziente Wärmenetze.” 2019, Accessed: Feb. 04, 2021. [Online]. Available: <https://www.bundesanzeiger.de/pub/publication/iWrOAbNtQ7qTa0GkMrh/content/iWrOAbNtQ7qTa0GkMrh/BAnz%20AT%2024.12.2019%20B1.pdf?inline>.
- [28] Bundesamt für Wirtschaft und Ausfuhrkontrolle, “Modellvorhaben Wärmenetzsysteme 4.0 - Modul II: Antragstellung und Verwendungsnachweis.” 2019, Accessed: Feb. 04, 2021. [Online]. Available: https://www.bafa.de/SharedDocs/Downloads/DE/Energie/wns_4_m2_merkblatt_realisierung.pdf?__blob=publicationFile&v=7.
- [29] P. Remmen, M. Lauster, M. Mans, M. Fuchs, T. Osterhage, and D. Müller, “TEASER: An open tool for urban energy modelling of building stocks,” *Journal of Building Performance Simulation*, vol. 11, no. 1, pp. 84–98, 2018, <https://doi.org/10.1080/19401493.2017.1283539>.
- [30] T. Loga, N. Diefenbach, B. Stein, and R. Born, “TABULA – scientific report germany – further development of the german residential building typology.” Darmstadt, 2012, Accessed: Feb. 04, 2021. [Online]. Available: https://episcopes.eu/fileadmin/tabula/public/docs/scientific/DE_TABULA_ScientificReport_IWU.pdf.
- [31] A. Kallert, R. Egelkamp, and D. Schmidt, “High resolution heating load profiles for simulation and analysis of small scale energy systems,” *Energy Procedia*, vol. 149, pp. 122–131, 2018, <https://doi.org/10.1016/j.egypro.2018.08.176>.
- [32] A. David, B. V. Mathiesen, H. Averfalk, S. Werner, and H. Lund, “Heat roadmap europe: Large-scale electric heat pumps in district heating systems,” *Energies*, vol. 10, no. 4, p. 578, 2017, <https://doi.org/10.3390/en10040578>

- [33] VDI 4640-2:2019-6, *Thermische Nutzung des Untergrunds - Erdgekoppelte Wärmepumpenanlagen*. 2019. [Online]. Available: <https://www.vdi.de/richtlinien/details/vdi-4640-blatt-2-thermische-nutzung-des-untergrunds-erdgekoppelte-waermepumpenanlagen>
- [34] U. Dehner, U. Müller, and J. Schneider, *Erstellung von Planungsgrundlagen für die Nutzung von Erdwärmekollektoren*. Hanover, Germany: Landesamt für Bergbau, Energie und Geologie, 2007. [Online]. Available: https://www.lbeg.niedersachsen.de/download/1220/GeoBerichte_5.pdf
- [35] T. Huld, R. Müller, and A. Gambardella, "A new solar radiation database for estimating PV performance in europe and africa," *Solar Energy*, vol. 86, no. 6, pp. 1803–1815, 2012, <https://doi.org/10.1016/j.solener.2012.03.006>.
- [36] E. Dunkelberg et al., "Keimzellen für eine Quartierswärmeversorgung. Abwasserwärmenutzung durch Gebäude einer städtischen Wohnungsbaugesellschaft in einem Berliner Bestandsquartier, Arbeitsbericht 1." Berlin, 2020, Accessed: Feb. 04, 2021. [Online]. Available: https://www.ioew.de/fileadmin/user_upload/BILDER_und_Downloaddateien/Publikationen/2020/Dunkelberg_et_al_2020_Keimzellen_fuer_Quartierswaermeversorgung.pdf.
- [37] E. Dunkelberg et al., "Fernwärme klimaneutral transformieren - Eine Bewertung der Handlungsoptionen am Beispiel Berlin Nord-Neukölln." Berlin, 2020, Accessed: Feb. 04, 2021. [Online]. Available: https://www.ioew.de/fileadmin/user_upload/BILDER_und_Downloaddateien/Publikationen/Schriftenreihen/IOeW_SR_218_Fernwaerme_klimaneutral_transformieren.pdf.
- [38] P. Østergaard, R. Johannsen, H. Lund, and B. Mathiesen, "Latest developments in 4th generation district heating and smart energy systems," *Int J Sustain Energy Plan Manag*, 2021, <https://doi.org/10.5278/ijsepm.6432>.

